END

FILMED

DTIC

MICROCOPY RESOLUTION TEST CHART

NATIONAL BUREAU OF STANDARDS-1963-A

⑬

Design of an Optical Proximity Sensor Using Multiple Cones of Light for Measuring Surface Shape

Michael Fuhrman and Takeo Kanade

Carnegie-Mellon University
The Robotics Institute

Technical Report

FEB 07 1985

E

85   01   28   148

Design of an Optical Proximity Sensor
Using Multiple Cones of Light for
Measuring Surface Shape

Michael Fuhrman and Takeo Kanade

CMU-RI-TR-84-17

The Robotics Institute
Carnegie-Mellon University
Pittsburgh, Pennsylvania 15213

April 1984

DTIC

SECURITY CLASSIFICATION OF THIS PAGE (When Data Entered)

REPORT DOCUMENTATION PAGE	READ INSTRUCTIONS BEFORE COMPLETING FORM

1. REPORT NUMBER	2. GOVT ACCESSION NO	3. RECIPIENT'S CATALOG NUMBER
CMU-RI-TR-84-17	AD-A150050	

4. TITLE (and Subtitle)	5. TYPE OF REPORT & PERIOD COVERED
Design of an Optical Proximity Sensor Using Multiple Cones of Light for Measuring Surface Shape	Interim
	6. PERFORMING ORG. REPORT NUMBER

7. AUTHOR(s)	8. CONTRACT OR GRANT NUMBER(s)
Michael Fuhrman and Takeo Kanade	ONR N00014-81-K-0503

9. PERFORMING ORGANIZATION NAME AND ADDRESS	10. PROGRAM ELEMENT, PROJECT, TASK AREA & WORK UNIT NUMBERS
Carnegie-Mellon University The Robotics Institute Pittsburgh, PA. 15213	

11. CONTROLLING OFFICE NAME AND ADDRESS	12. REPORT DATE
Office of Naval Research Arlington, VA 22217	April 1984
	13. NUMBER OF PAGES
	24

14. MONITORING AGENCY NAME & ADDRESS(If different from Controlling Office)	15. SECURITY CLASS. (of this report)
	UNCLASSIFIED
	15a. DECLASSIFICATION/DOWNGRADING SCHEDULE

16. DISTRIBUTION STATEMENT (of this Report)

Approved for public release; distribution unlimited

17. DISTRIBUTION STATEMENT (of the abstract entered in Block 20, if different from Report)

Approved for public release; distribution unlimited

18. SUPPLEMENTARY NOTES

19. KEY WORDS (Continue on reverse side if necessary and identify by block number)

20. ABSTRACT (Continue on reverse side if necessary and identify by block number)

A noncontact multi-light source optical proximity sensor which can measure the distance, orientation, and curvature of a surface has been developed. Beams of light are sequentially focused from the ends of fiber optic cables onto a target surface. An analog light-sensor - a planar PIN diode area sensor chip - measures the position of the spots of light on the surface, and the 3-D locations of the spots are computed by triangulation. By fitting a surface to a set of points, the distance, orientation and curvature of the target surface is calculated. The number of light sources, and their positions and orientations were chosen so that the uncertainty

DD FORM 1 JAN 73 1473   EDITION OF 1 NOV 65 IS OBSOLETE
S/N 0102-014-6601 |

UNCLASSIFIED
SECURITY CLASSIFICATION OF THIS PAGE (When Data Entered)

(20. cont'd.)

in the measurement of distance would be within 0.05 mm and the uncertainty in surface orientation would be within 1.0°

Since there are no moving parts and the spot position sensor chip outputs the position of the spot directly without scanning its field of view, fast operation of the proximity sensor can be realized. Earlier prototype versions of the sensor can give approximately 1000 measurements of distance and orientation per second with precision of 0.07 mm for distance and 1.5° for surface orientation. This proximity sensor will be useful for such applications as tracing an object surface by a robot manipulator with a specified distance and orientation relative to the surface.

Table of Contents

Abstract

A noncontact multi-light source optical proximity sensor which can measure the distance, orientation, and curvature of a surface has been developed. Beams of light are sequentially focused from the ends of fiber optic cables onto a target surface. An analog light sensor - a planar PIN diode area sensor chip - measures the position of the spots of light on the surface, and the 3-D locations of the spots are computed by triangulation. By fitting a surface to a set of points, the distance, orientation and curvature of the target surface is calculated. The number of light sources, and their positions and orientations were chosen so that the uncertainty in the measurement of distance would be within 0.05 mm and the uncertainty in surface orientation would be within 1.0°.

Since there are no moving parts and the spot position sensor chip outputs the position of the spot directly without scanning its field of view, fast operation of the proximity sensor can be realized. Earlier prototype versions of the sensor can give approximately 1000 measurements of distance and orientation per second with precision of 0.07 mm for distance and 1.5° for surface orientation. This proximity sensor will be useful for such applications as tracing an object surface by a robot manipulator with a specified distance and orientation relative to the surface.

1. Introduction

Noncontact proximity sensors which can measure the range and shape of a surface have useful robotic applications such as surface tracking and homing a manipulator to an object. The proximity sensor we have developed can measure the distance, orientation, and curvature of a surface, along with surface properties such as reflectivity. Because the focus of the proximity sensor is on a small area of surface, measurements can be fast and precise.

Many optical proximity sensors have been built. The simplest sensors use the sensitive-volume technique [1]. A beam of light originating from a sensor's light source illuminates a surface. The closer the surface is to the sensor, the greater the intensity of the reflected light reaching the sensor. This technique is sensitive not only to the distance of a surface, but also to its orientation and reflectivity. One way to overcome these sensitivities is to use several light sources and compare the relative intensities of the reflected light to measure distance [7].

Our proximity sensors differ from other proximity sensors in that they are based on triangulation, that they use an analog light sensor with two-dimensional spatial resolution, and that they exploit redundant multiple light sources to increase accuracy. The fast, high spatial-resolution light sensor chip provides the proximity sensor with the capability of accurate and fast measurement of light spot position. The multiple light sources enable the sensor to measure surface orientation and surface curvature, and to measure distance with increased accuracy by virtue of its geometrical redundancy.

This paper first discusses a basic model of the multiple light source proximity sensor. This model enables us to calculate the necessary number of light sources and their appropriate orientations to achieve a specified accuracy when measuring distance and orientation. After presenting the results of earlier prototypes of the sensor we present a new proximity sensor with a range of 10.0 cm, and a precision better than 0.05 mm for distance and $1.0°$ for surface orientation.

2. Measurement of Distance and Shape

2.1. Overview

Figure 1 shows the basic configuration of the type of proximity sensor we are developing. The sensor head consists of a ring of light sources, a camera lens, and a light-spot position sensor chip. The light sources focus beams of light towards a point along the optical axis of the sensor. The precise geometry of the sensor is determined by its required range and resolution.

The arrangement of the lens and spot position detector is basically that of a camera. One light source is

turned on at a time. When a target surface interrupts a light beam, the resultant light spot is imaged onto the sensor chip through the lens. The sensor chip then measures the spot position on its active two-dimensional face. Knowledge of the spot position on the sensor chip, together with the camera optics, and the trajectory of each light beam, allow us to perform triangulation in order to determine the three-dimensional coordinates of each light spot on the target surface. From the measurement of multiple points in the field of view, the orientation and curvature of the surface can be calculated. In addition, since the sensor chip also measures the intensity of light incident on its surface, we can calculate the reflectivity of the target surface.

The sensor chip which detects the light reflected from a surface is an analog device. The chip, a planar PIN diode, measures both the intensity of the light which strikes it and the position of the light spot on its surface [3]. If the spot of light on a surface is distorted because of the curvature or orientation of the surface, or if the spot is out of focus, the sensor chip still responds to the stimulus with coordinates corresponding to the centroid of the light spot. Together with the fast response time, this feature has advantages over an imaging device composed of discrete pixels (such as a CCD camera), which would require computation to find the centroid of the light spot. To minimize the error in the measurement the light spot size must still be kept to a minimum. To achieve this capability in the proximity sensor we are building, each light source will focus light emitted from the end of fiber optic cable. In this way the light spot size can be kept on the order of the size of the fiber core.

2.2. Measuring the Distance of a Surface

The trajectory of each light beam which illuminates a surface is fixed and can be calibrated in advance, and the line of sight to the light spot is obtained from the sensor chip. The calculation of the coordinates of a spot of light on a surface by triangulation is based on a simple optical model: first, the light source beam is a line, and thus the projected light spot is a point; second, the camera lens forms a flat, undistorted image; and finally the sensor chip is linear in finding the light spot position and is insensitive to defocus. Of course, the sensor is subject to small errors because of deviations from the simple model. However since the errors are small and fixed over time, we treat them as perturbations from the model and calculate error correction terms beforehand.

The position and orientation of a line in 3-D space can be defined by the coordinates of a point on the line and the direction cosines of the line. In Figure 2 the line of light beam is defined by the light source origin $\vec{P}_s = (x_s, y_s, z_s)$ and the light beam direction vector $\vec{A}_s = (a_s, b_s, c_s)$. The line of sight has an orientation $\vec{A}_o = (a_o, b_o, c_o)$ which is defined by the camera lens center $\vec{P}_o = (x_o, y_o, z_o)$ and the centroid of the spot of light (x_c, y_c) on the sensor chip. Let us denote the coordinate of the spot position we want to locate as $\vec{P} = (x, y, z)$. In theory, the two three-dimensional lines (the light source beam and the line of sight) should intersect at the location of the spot on the surface. In reality, however, the two spatial lines thus obtained only

come very close due to noise and the simplified optical model being used. We therefore determine the spot location $\vec{P}$ to be located along the line of closest approach (i.e., along the common normal) between the two skew lines. The direction of the common normal is $\vec{\Lambda} = \vec{\Lambda}_s \times \vec{\Lambda}_o$. By noticing that $\vec{P}$ is on the common normal, we obtain the following equations:

$$
\begin{aligned}
(\vec{P} - \vec{P}_s)\cdot(\vec{\Lambda}_s \times \vec{\Lambda}) &= 0, \\
(\vec{P} - \vec{P}_o)\cdot(\vec{\Lambda}_o \times \vec{\Lambda}) &= 0, \\
(\vec{P} - \vec{P}_o)\cdot\vec{\Lambda} &= \lambda(\vec{P}_s - \vec{P}_o)\cdot\vec{\Lambda}.
\end{aligned}
\tag{1}
$$

The first two equations define the intersection of two planes along the common normal of the two skew lines. The factor λ in the third equation determines where $\vec{P}$ is located along the common normal depending on which of the two spatial lines are more reliable. In our sensor we have chosen λ to be 1.0, that is, $\vec{P}$ falls by definition on the line of the light source beam. By solving the above simultaneous linear equations, we obtain the spatial location of a spot on the surface for each light source.

As already mentioned, we assume a line of sight can be drawn from the image of the light spot on the sensor chip through the effective center of the lens towards the light spot on the surface. The distance between the effective center of the lens and the sensor chip cannot be measured directly. Instead, a flat surface is brought into focus on the sensor chip at a typical distance D from the sensor chip. Then the distance i between the sensor chip and the effective center of the lens is calculated in terms of the focal length f of the lens and the distance D:

$$
\frac{1}{i} + \frac{1}{D - i} = \frac{1}{f},
$$

$$
i = \frac{D}{2}(1 - \sqrt{1 - 4f/D}).
\tag{2}
$$

2.3. Surface Fitting

To estimate the position and orientation of a surface, a plane is fit to the set of three dimensional data points obtained by the proximity sensor. To estimate the curvature of a surface, a second order equation is fit. The accuracy of the calculation of position, orientation and curvature depends, therefore, on the accuracy of the individual data points, and the number and distribution of the data points on the surface. For example, if the points are too closely spaced, the orientation of the plane which is fit to the points will be very uncertain. We will analyze these relationships and use the results to design a sensor whose expected uncertainties are less than the design specifications.

Let us suppose that we have n measured points on a surface, where each point (x_i, y_i, z_i) has an estimated total uncertainty in position of σ_i. A surface can be fit to this set of points using the method of least squares to determine the coefficients a_j in the equation

$$z(x, y) = \sum a_j X_j(x, y) \tag{3}$$

where $X_j(x, y)$ is a polynomial of the form $\sum c_{qr} x^q y^r$. For example, when fitting a plane, $q + r \leq 1$, and when fitting a quadric surface, $q + r \leq 2$. We are concerned with how the uncertainty in the measured points and their distribution on the surface affects the uncertainty of the computed coefficients.

The values of the coefficients a_j are chosen so that they minimize the aggregate error E:

$$E = \sum_{i=1}^{n} \{ \frac{1}{\sigma_i^2}(z_i - z(x_i, y_i))^2 \} = \sum_{i=1}^{n} \{ \frac{1}{\sigma_i^2}(z_i - \sum a_j X_j(x_i, y_i))^2 \}. \tag{4}$$

By minimizing E, each a_j can be computed by:

$$a_j = \sum_k e_{jk} \beta_k \tag{5}$$

where $[e_{jk}] = [\alpha_{jk}]^{-1}$ \tag{6}

$$\alpha_{jk} = \sum_{i=1}^{n} \{ \frac{1}{\sigma_i^2} X_j(x_i, y_i) X_k(x_i, y_i) \} = \frac{1}{2} \frac{\partial^2 E}{\partial a_j \partial a_k} \tag{7}$$

$$\beta_k = \sum_{i=1}^{n} \{ \frac{1}{\sigma_i^2} z_i X_k(x_i, y_i) \}. \tag{8}$$

The symmetric matrix $[\alpha_{jk}]$ is known as the curvature matrix because of its relationship to the curvature of E in the coefficient space [2].

We can estimate the uncertainties of the coefficients, and determine their dependence on the geometry of the proximity sensor if we assume that fluctuations in the coordinates of the individual data points are uncorrelated, and assign the total uncertainty in the measurement of position to the variable z. The uncertainty of the coefficient a_j is then

$$\sigma_{a_j}^2 = \sum_{i=1}^{n} \sigma_i^2 \left(\frac{\partial a_j}{\partial z_i} \right)^2. \tag{9}$$

By calculating the partial derivatives of equation (5), it follows that the uncertainties of the coefficients are proportional to the diagonal elements of the inverse of the curvature matrix [2], that is

$$\sigma_{a_j}^2 = e_{jj} \tag{10}$$

Let us first examine the case where the plane

$$z = Gx + Hy + I \qquad (11)$$

is fit to a set of data points. Here we have set $a_1 = G$, $a_2 = H$, $a_3 = I$, $X_1 = x$, $X_2 = y$, and $X_3 = 1$ in equation (3). The local surface normal is $\vec{N} = (G, H, -1)$. Since all of the measured points on a surface are at about the same distance from the sensor in any one measurement cycle, the total uncertainty σ_i can be taken as a constant σ for all of the data points. The curvature matrix for this case is

$$\alpha = \frac{1}{\sigma^2} \begin{pmatrix} \Sigma x_i^2 & \Sigma x_i y_i & \Sigma x_i \\ \Sigma x_i y_i & \Sigma y_i^2 & \Sigma y_i \\ \Sigma x_i & \Sigma y_i & n \end{pmatrix} . \qquad (12)$$

In many applications the proximity sensor will be used to maintain an orientation normal to a surface. The light sources can be arranged symmetrically so that the resulting spots of light on a flat surface facing the sensor perpendicularly satisfy the condition

$$\Sigma x_i = \Sigma y_i = \Sigma x_i y_i = 0 \qquad (13)$$

that is, the α matrix is diagonal. The uncertainties in the coefficients of equation (11) are then simply

$$\sigma_G = \frac{\sigma}{\sqrt{\Sigma x_i^2}},$$

$$\sigma_H = \frac{\sigma}{\sqrt{\Sigma y_i^2}}, \qquad (14)$$

$$\sigma_I = \frac{\sigma}{\sqrt{n}}.$$

The angle between the optical axis of the proximity sensor and the surface normal is $\varphi = \operatorname{atan} \sqrt{G^2 + H^2}$. The uncertainty in the angular orientation of a surface perpendicular to the sensor can be estimated by

$$\sigma_\varphi{}^2 \leq \sigma_G{}^2 + \sigma_H{}^2. \qquad (15)$$

Equations (14) and (15) then, relate the uncertainty in the measured position and orientation of a surface with the number of data points, the uncertainty in their measurement, and their distribution on the surface.

A proximity sensor which measures surface curvature can be used, for example, to track the edge of an object, guided by the principal axes of curvature. The radii of curvature provide useful information for

maintaining a constant distance and orientation with respect to a surface. To calculate surface curvature, a second order equation

$$z = Ax^2 + Bxy + Cy^2 + Dx + Ey + F \qquad (16)$$

is fit to the set of data points. The principal axes of curvature are at an angle

$$\psi = \frac{1}{2}\cot^{-1}\frac{A-C}{B} \qquad (17)$$

with respect to the x-y coordinate axes.

Equation (16) can be transformed by rotating the coordinate axes to eliminate the cross term, and translating the coordinate axes to eliminate the linear terms. In this new coordinate system the equation of the surface is

$$z = A'x'^2 + C'y'^2 + F'.$$

The principal normal curvatures κ_1 and κ_2 of the surface are given by

$$\frac{\kappa_1}{2} = A' = A\cos^2\psi + B\sin\psi\cos\psi + C\sin^2\psi,$$

$$\frac{\kappa_2}{2} = C' = A\sin^2\psi - B\sin\psi\cos\psi + C\cos^2\psi. \qquad (18)$$

The uncertainty in the measured curvature of a surface is given by

$$\sigma^2_{\kappa_1} = 4\sigma^2_{A'}$$

$$\sigma^2_{\kappa_2} = 4\sigma^2_{C'}$$

The uncertainty in the orientation of the principal axes σ_ψ can be estimated by

$$\sigma_\psi^2 = \sigma_A^2\left(\frac{\partial\psi}{\partial A}\right)^2 + \sigma_B^2\left(\frac{\partial\psi}{\partial B}\right)^2 + \sigma_C^2\left(\frac{\partial\psi}{\partial C}\right)^2 = \frac{1}{4}\frac{\sigma_B^2}{(A'-C')^2}. \qquad (19)$$

This means that the ability of the sensor to detect the principal axes of curvature depends on the difference $A' - C'$ between the principal curvatures of the surface; or in other words, the eccentricity of the surface which is fit to the data points.

Fitting the second order (and higher) equation of a surface to a set of data points requires practical consideration because of the finite word length of the computer. The computation of the coefficients of higher order terms is dependent on the computation of lower order coefficients, and the results can be inaccurate. The appropriate method for removing the interdependence of the coefficients is to first calculate a set of polynomials $X_j(x, y)$ which are orthogonal to each other over the set of data points and then perform a

least squares fit using the orthogonal polynomials [2, 4]. The coefficients of equation (16) are then found by regrouping terms of corresponding order.

2.4. Error Correction

As we have mentioned, the optical model used so far includes a few simplifications. Because of the existence of various distortions and nonlinearities in the sensor chip, the optics and the electronics, the calculation of the spatial location $\vec{P} = (x, y, z)$ of the spot using equation (1) includes errors. Suppose that $(\tilde{x}, \tilde{y}, \tilde{z})$ is the correct location. Let us set

$$
\begin{aligned}
\tilde{x} &= x + \varepsilon_x \\
\tilde{y} &= y + \varepsilon_y \\
\tilde{z} &= z + \varepsilon_z.
\end{aligned}
$$

It would be very difficult to model the effect of the departures from the simplified model precisely to determine the terms ε_x, ε_y, and ε_z. However, since the errors are small and usually repeatable with respect to the measured spot position (x_c, y_c) on the sensor chip, we can model them as a whole by means of polynomials, for example, by third order correction polynomials of the form

$$
\begin{aligned}
\varepsilon_t = f_t(x_c, y_c) = {}& a_{t1}x_c^3 + a_{t2}x_c^2 y_c + a_{t3}x_c y_c^2 + a_{t4}y_c^3 \qquad (20) \\
& + a_{t5}x_c^2 + a_{t6}x_c y_c + a_{t7}y_c^2 \\
& + a_{t8}x_c + a_{t9}y_c + a_{t10}
\end{aligned}
$$

where $t = x,y,z$.

When the proximity sensor is calibrated, these polynomials are designed for each LED using a calibrated data set. During operation, the values ε_x, ε_y, and ε_z computed by equations (20) are added to the spatial coordinates (x, y, z) computed by triangulation to obtain the corrected location of the spot.

3. Early Multi-light Source Proximity Sensors

Two prototype versions of the proximity sensor were built to test the basic principles of sensor operation, and the usefulness of the analog sensor chip. The first version of the sensor used six infrared LEDs oriented in a conical pattern at a 45° angle, all aimed towards a point on the optical axis 4.5 cm from the sensor chip [5, 6]. The distance of this point from a simple lens was equal to the distance of the lens from the sensor chip. Hence the area of the field of view over the range of the sensor was about equal to the size of the sensor chip, or 13 mm square. The range of measurement depth of the sensor was ±5.6 mm. Because all of the light sources were focused towards one point, the orientation of the plane fit to the data points on a surface located at this singular point was not accurate.

The second version of the proximity sensor, shown in Figure 3, was designed so that the light source positions could be measurably adjusted, and standard camera lenses could be used. This sensor covered a

larger range of ±2.5 cm, centered about a point approximately 10 cm from the sensor chip. To ensure that the field of view would be much larger than the spots of light on a surface, an area four times the linear dimensions of the sensor chip was brought into focus. Instead of a single cone of light, two cones were formed: three light sources were focused towards one point on the optical axis, and three others towards a second point 0.5 cm beyond the first. In this way, the singularity which occurred in the first version was removed. The proximity sensor could measure surface orientation throughout its range. Again, all of the light sources were oriented at a 45° angle.

3.1. Performance

In order to measure the accuracy and sensitivity of the proximity sensors, a flat test surface was moved linearly and rotated by high resolution platforms in the sensors' field of view. The equation of a plane fit to the six measured spatial points on the test plane was compared with the known equation of the test plane. The error in measured distance was taken as the difference between the points where the two planes intersected the optical axis. The error in orientation was evaluated by the angle made by the surface normals of the two planes.

The position and orientation errors for the second version of the sensor with all of its light sources focused towards a single point are displayed in Figures 4(a) and 4(b) as a function of the distance and orientation of the test surface. *In this particular configuration the sensor had a useful range of about ±1.25 cm.* The height of each graph shown is proportional to the measurement error. The distance and orientation of the surface was varied in .254 mm and 1° steps. The singularity at the distance $d = 50$ where the beams of light converge is evident in both figures. Near $d = 0$ where the test surface was very close to the sensor, and near $d = 100$ where the surface was further away, the light source beams enter and leave the field of view. These are the boundaries of the sensor's useful range. The results of these tests for both sensors showed a central region where the error in orientation was typically less than 1.5°, and the overall error in the measurement of distance was less than 0.07 mm.

As the test surface facing the proximity sensor perpendicularly was moved from $d = 0$ to $d = 100$ along the optical axis, the light spots traced individual paths on the surface. The trajectories of the x and y coordinates of the light spots on the surface are displayed in Figure 5. The endpoints of the trajectory of light source number 4 are labeled in the figure. As has been mentioned, when a surface is close to the sensor the light spot projected by a light source can fall partly outside of the field of view. As a result, the calculation of the light spot position for a light source can be in error. This effect is seen in the deviation of the trajectory of light source number 5. However because multiple light sources are used, several light spots can always be focused in the center of the field of view. In this way, accurate position information about a set of points can always be acquired.

Although their performance was good, the usefulness of these earlier versions of the sensor was limited by several factors: first, the range of distance measurement was not long enough; second, the total number of light sources was not large enough to ensure high accuracy; third, the size of the light spots which they projected onto a surface was not small; and finally, these sensors were not compact enough to be mounted on a robotic manipulator. In the following discussion we outline the design of a new proximity sensor using multiple conical arrays of light sources. In addition to making the sensor compact, the design method is based on the statistical discussion of the previous section, and takes into account the resolution of the sensor chip, the number and orientations of the light sources, and the desired range and resolution of the final sensor.

4. The Design of a Sensor using Multiple Conical Arrays

Uncertainty in the measurement of surface orientation ultimately depends upon the uncertainty with which the sensor chip measures light spot position. Although the resolution of the sensor chip is potentially high (about 1/5000 across its surface), the precision of a single measurement is limited by several factors. The intensity of the light which reaches the sensor chip depends upon the distance, orientation and reflectivity of the measured surface. The shape of a surface also affects the intensity distribution of the light spot on the sensor chip, causing a small error in measurement. However because the sensor chip is very fast, we can use redundant multiple light sources and choose the orientations and positions of the light sources so as to increase the accuracy of the sensor.

When measuring the distance of a surface, the region of greatest interest is generally the center of the sensor's field of view. The effects of the various distortion and non-linearity are smallest near the optical axis. In addition, even if a spot of light is out of focus or grossly distorted by a surface, errors which are the result of a portion of the light spot falling beyond the edge of the sensor chip will be minimized. For these reasons the proximity sensor is configured using multiple conical arrays of light sources. In this way, several light sources are always focused near the optical axis over the range of the sensor.

Since the sensor chip measures the centroid of the intensity distribution on its surface, the distortion of the spot of light on a flat surface does not lead to an appreciable error. However, a large light spot size does decrease the linear range of the proximity sensor, and certainly will affect the measurement of curved surfaces. To minimize the size of the light spots, the new design will use narrow core fiber optic cables. Use of narrow core fiber optic cable lets us generate a point light source which we can focus using a simple lens without having to worry about the size or shape of the original light emitter. Also, there is no intervening material, such as the micro-lens on an LED, to scatter light and form an image of an entire light source on the target surface. The light emitters can be positioned remotely and, during adjustment, the fiber cables can be coupled temporarily to a visible light source such as a laser to facilitate focusing and alignment.

4.1. Placement and Orientation of Conical Arrays

Having decided that all of the light sources are to be arranged in multiple conical arrays, we first determine the angles of orientation for these light sources, and then the number of light sources comprising each cone, the number of cones, and the placement of the cones by means of the statistical analyses of errors.

Figure 6 shows the locations of the sensor chip, the lens, and one light source focused on a point along the optical axis. The angle of the light beam relative to the x axis is θ. A line is drawn from the point on a surface interrupting the light beam, through the effective center of the lens, to the sensor chip. The equation of the beam of light in the x-z plane is

$$z = x \tan\theta + d. \tag{21}$$

The x coordinate of the spot of light on the sensor chip is

$$x_c = -\frac{L}{z - L} x. \tag{22}$$

A small change in the z coordinate of the target surface by Δz corresponds to a shift in the spot of light on the sensor chip by Δx_c:

$$S = \frac{\Delta x_c}{\Delta z} = -\frac{L}{(z - L)\tan\theta} + \frac{L(z - d)}{(z - L)^2 \tan\theta}. \tag{23}$$

The larger the magnitude of S, the more sensitive the measurement. The orientation of the light beam θ can be chosen so any measurement of distance using a single light source will have a nominal sensitivity S_N in the center of the field of view, i.e., at $z = d$. This condition places an upper bound on the value of θ:

$$\theta < \arctan\left[\frac{L}{(d - L)}\frac{1}{S_N}\right]. \tag{24}$$

Suppose one particular cone of light is generated using n light sources equally spaced in a circle. When a flat surface intersects the cone of light beams normal to the axis of the cone, the spots of light fall on a circle. The radius R of the circle is given by

$$R = |z - d|\cot\theta. \tag{25}$$

To determine the uncertainty in the orientation of a plane which is fit to these points, the mean-square values of the coordinates are first calculated.

$$\sum_{i=1}^{n} x_i^2 = R^2 \sum_{i=1}^{n} \cos^2 \frac{2\pi i}{n} = \frac{nR^2}{2} + \frac{R^2 \cos(2\pi/n) \sin 2\pi}{2 \sin(2\pi/n)}$$

$$\sum_{i=1}^{n} y_i^2 = R^2 \sum_{i=1}^{n} \sin^2 \frac{2\pi i}{n} = \frac{nR^2}{2} - \frac{R^2 \cos(2\pi/n) \sin 2\pi}{2 \sin(2\pi/n)}. \tag{26}$$

When $n \geq 3$ both of these expressions converge to $nR^2 / 2$. Using equations (14) and (15), the uncertainty in measured orientation when using a single cone of light can be calculated in terms of the uncertainty σ in the measurement of spot position, the radius of the circle of points and the number of light sources.

$$\sigma_\varphi \leq \frac{\sigma}{R} \frac{2}{\sqrt{n}} \tag{27}$$

When using multiple cones of light, where the jth cone consists of n_j light sources focused towards a point d_j, the radius of the jth cone at z is

$$R_j = |z - d_j| \cot \theta_j \tag{28}$$

The mean square value of the x coordinates of the data points is then

$$\sum_{i} x_i^2 = \frac{1}{2} \sum_{j} n_j \cot^2 \theta_j (z - d_j)^2. \tag{29}$$

The uncertainty in measured orientation becomes

$$\sigma_\varphi \leq \frac{2\sigma}{\sqrt{\sum n_j \cot^2 \theta_j (z - d_j)^2}}. \tag{30}$$

This equation guides the determination of the number of light sources n_j in each cone, their orientation θ_j and their placement d_j.

4.2. The New Proximity Sensor

The design of the new proximity sensor is guided by several design goals: the sensor should be compact, with dimensions on the order of 10 cm, in order that it can be used by a robotic manipulator; the sensor should have a useful range of about 10 cm; the incident angle of the light beams on a target surface should be small to minimize light spot distortion; there should be at least three separate conical rings of light sources; and each individual light source should measure position with a sensitivity of at least 0.25 mm.

The major constraint on the design of the proximity sensor is the light source intensity. The intensity of the light which is incident on a target surface depends on the intensity of the light emitter, the diameter of the fiber optic cable, and the diameter and focal length of the focusing lenses. These last two quantities determine the size of the sensor and the number of light sources which can be mounted on the sensor head. The intensity of the reflected light which reaches the sensor chip depends on the distance of the camera lens from the target surface and the diameter of the lens.

In a tradeoff between sensitivity, range, and the size of the field of view, the distance from the camera lens to the plane which is in best focus was chosen to be 3.42 times the distance from the sensor chip to the lens. As a result, the area of the field of view which is in best focus is approximately 4.0 cm square. In the new version of the sensor we use a 16mm, f/1.6 camera lens. A camera lens with a shorter focal length would allow us to build a smaller sensor focused at a closer range with a wider field of view, but at the expense of losing long range sensitivity as the field of view rapidly expands. If we used a longer focal length camera lens the angular field of view would be smaller, and the sensitivity greater, but it is difficult to focus small spots of light with sufficient intensity at the greater distance which would then be in focus.

Figure 7 shows the configuration of the proximity sensor we are currently building. To begin the analysis, we choose three cones of light each consisting of three light sources. Equation (24) determines the choice of the angle of orientation of the light sources. With this angle chosen, we use equation (30) to calculate the minimum spacing between the vertices d_1, d_2 and d_3 of the cones of light, where $z = d_2$ is in best focus.

First we have to estimate the uncertainty σ in the measurement of spot position at $z = d_2$. Referring to equation (23) and equation (24), we first set $\theta = 60^\circ$, and $(d_2 - L) / L = 3.42$ and find $S_N = 6.67$. A smaller angle would increase the sensitivity of the sensor, but the light spot on a surface would then be further elongated. We assume that when a flat surface is measured, a signal to noise ratio can be achieved so that the effective resolution of the sensor chip is at least 1/500 its linear dimensions. This corresponds to $\Delta x_c = .026$ mm, and a shift in the position of the target surface by $\Delta z = .15$ mm. This value of Δz is used to estimate σ_z. The total uncertainty σ is estimated by observing that when the position of a point is calculated by triangulation, the solution is constrained to lie on the line determined by the light beam. Since $\sigma^2 \approx \sigma_x^2 + \sigma_y^2 + \sigma_z^2$, and $\tan 60^\circ = \sqrt{3}$,

$$\sigma_z^2 \approx 3(\sigma_x^2 + \sigma_y^2)$$

so

$$\sigma^2 \approx 1.33\sigma_z^2.$$

The maximum value of the uncertainty in the measurement of surface orientation σ_φ occurs near at the vertex of the middle cone. We use equation (30) to calculate the minimum spacing between the vertices d_1, d_2 and d_3 of the cones of light by insisting the uncertainty in any single measurement of orientation at $z = d_2$ be less than 1.0° (17.4 milliradians). Assuming these three cones are equally spaced, and consist of three light sources, we find

$$14.0 \text{ mm} \leq d_2 \cdot d_1 = d_3 \cdot d_2. \tag{31}$$

Figure 8 shows how the uncertainty in orientation σ_φ calculated by equation (30) decreases as cones of light are added to the proximity sensor head. $\sigma_\varphi(1)$ is graphed assuming a single cone of light consisting of three light sources is focused towards d_2. Then $\sigma_\varphi(2)$ and $\sigma_\varphi(3)$ are graphed as successive cones of light are added: first the cone with a vertex at d_3, then the cone with a vertex at d_1.

To further increase the accuracy of the sensor a second cone of light is focused at d_1 to augment the original light sources. In order to extend the range of the sensor, two more cones of light with an orientation of 70° are focused towards points further along the optical axis. As a result, the range of the proximity sensor consists of two overlapping regions: first an inner region with a small field of view, a depth of 6 cm, and many redundant light sources where the sensor accurately measures the distance and shape of a surface, and then an outer region which extends the range of the sensor by another 4 cm.

This new proximity sensor uses a total of 18 light sources arranged in 5 conical arrays. The overall accuracy in the measurement of position when using the innermost 12 light sources is expected to be on the order of .05 mm. The accuracy in the measurement of surface orientation is expected to be better than 1°. The diameter of the sensor is 11 cm across. To summarize, the final parameters of the proximity sensor are:

Camera lens focal length: $f = 16$ mm
Sensor chip to lens distance: $L = 20.67$ mm
Distance from sensor chip to plane in best focus: $D = 9.14$ cm
Orientation of inner rings of light sources: $\theta_{1,2,3} = 60^\circ$
Orientation of outer rings light sources: $\theta_{4,5} = 70^\circ$
Number of light sources in ring 1: $n_1 = 6$
Number of light sources in outer four rings: $n_{2,3,4,5} = 3$
Distance between inner light source target points along the optical axis: 15.24 mm

5. Conclusion

A new compact multi-light source proximity sensor has been developed. The sensor is based on the principle of active illumination and triangulation: each time a light source is pulsed, the coordinates of the resulting spot of the light on a surface are calculated. Two prototype proximity sensors have been built. The first was a very short range sensor with a precision of .07mm and $1.5°$ over a range of 40mm to 50mm. The second version has a range of 5cm. These prototypes acquired data at a rate exceeding 1000 points/second.

The design of a new version of the proximity sensor was guided by a statistical analysis of the uncertainty in the measurement of position using a single light source and the measurement of surface orientation using several light sources. The analysis related the number of light sources needed to measure orientation within a specified accuracy to the distribution of light spots on a target surface. The new design is also intended to be a compact sensor for use on a robotic manipulator.

The previous prototypes focused beams of light from LEDs to illuminate a surface. Although this method is useful and inexpensive, to accurately measure the orientation and curvature of a curved surface the sensor will have to project narrower beams of light onto a surface. To achieve this capability the new version of the sensor uses fiber optic cable to generate points of light in the field of view of the sensor.

The features of this proximity sensor include its simple principle of operation and fast speed. The sensor chip which detects the spot of light on the target surface is an analog device which outputs the position of the centroid of a spot of light on its surface. Although the accuracy of any individual measurement of light spot position is limited by the distortion of a spot of light by a surface, and the noise and sensitivity of the sensor, we take advantage of the speed of the sensor and use multiple light sources to increase the overall accuracy of measurements. The geometrical arrangement of the light sources was guided by the statistical analysis to achieve the design specification for accuracy. Measurement of distance, surface orientation and surface curvature can exploit the geometrical redundancy of the device.

Acknowledgements

References

[1] Bejczy, A.
Smart Sensors for Smart Hands.
Nasa Report Number 78-1714 , 1978.

[2] Bevington, Philip R.
Data Reduction and Analysis for the Physical Sciences.
McGraw-Hill Book Company, 1969.

[3] Hamamatsu TV Co. Ltd.
Photosensitive Devices: S1200 and S1300.
data sheet.

[4] Hayes, J.G.
Numerical Aproximation to Functions and Data.
Athlone Press, University of London, 1970.

[5] Kanade, T., Asada, H.
Noncontact Visual 3-D Sensing Devices.
In *SPIE Technical Symposium East '81, 3-D Machine Perception (Vol. 283).* Society of Photo-Optical
    Instrumentation Engineers, 1981.

[6] Kanade, T. and Sommer, T.
An Optical Proximity Sensor for Measuring Surface Position and Orientation for Robot Manipulation.
Technical Report TR-83-15, Carnegie Mellon University Robotics Institute, 1983.

[7] Okada, T.
A Short Rangefinding Sensor for Manipulators.
Bulletin of Electrotechnical Laboratory 42, 1978.
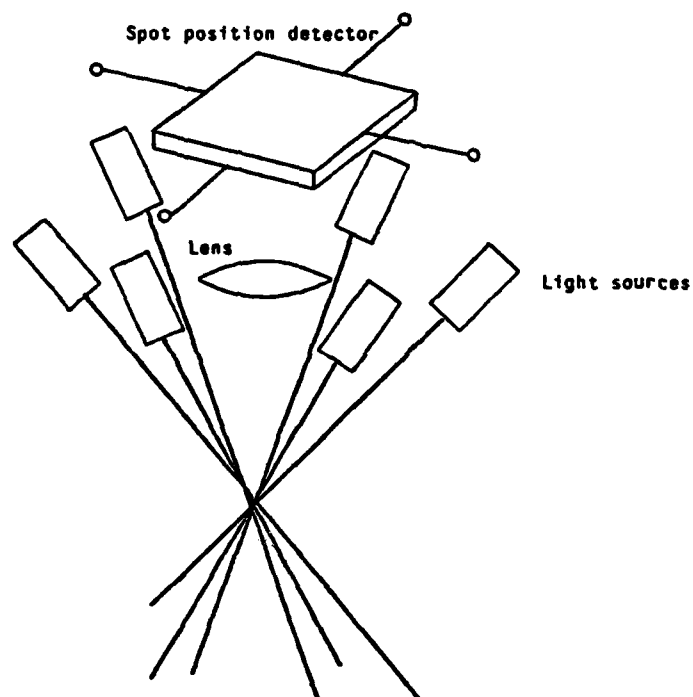
Figure 1: The multi-light source proximity sensor uses a position sensitive analog light sensor and multiple rings of infra-red light sources. The light sources in this sketch of a basic sensor are focused towards a point on the optical axis.
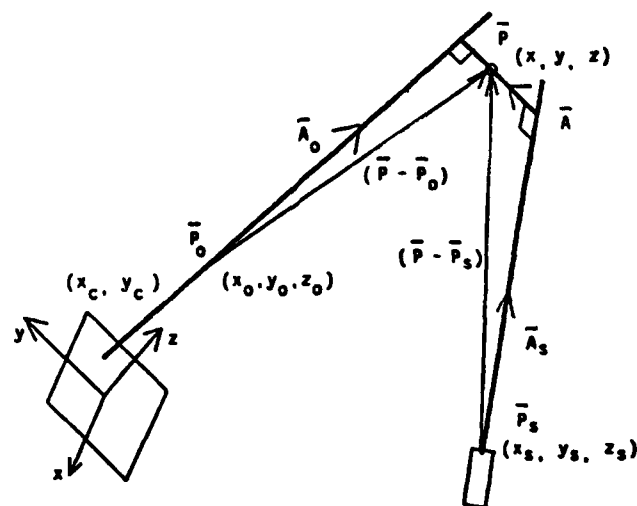
Triangulation:

$\bar{P}_0$: Center of the camera lens

$\bar{A}_0$: Vector defining the line of sight

$\bar{P}_s$: Location of light source

$\bar{A}_s$: Direction of light source

$\bar{P}$: The chosen result of triangulation

$\bar{A}$: A vector along the common normal

Figure 2: The coordinates of a spot of light on a target surface are calculated by triangulation. The direction of each light source beam is fixed. The sensor chip provides a line of sight towards the light spot. The location of P is determined by solving the simultaneous linear equations:

$$(\bar{P} - \bar{P}_s) \cdot (\bar{A}_s \times \bar{A}) = 0$$

$$(\bar{P} - \bar{P}_0) \cdot (\bar{A}_0 \times \bar{A}) = 0$$

$$(\bar{P} - \bar{P}_0) \cdot \bar{A} = \lambda (\bar{P} - \bar{P}_0) \cdot \bar{A}$$
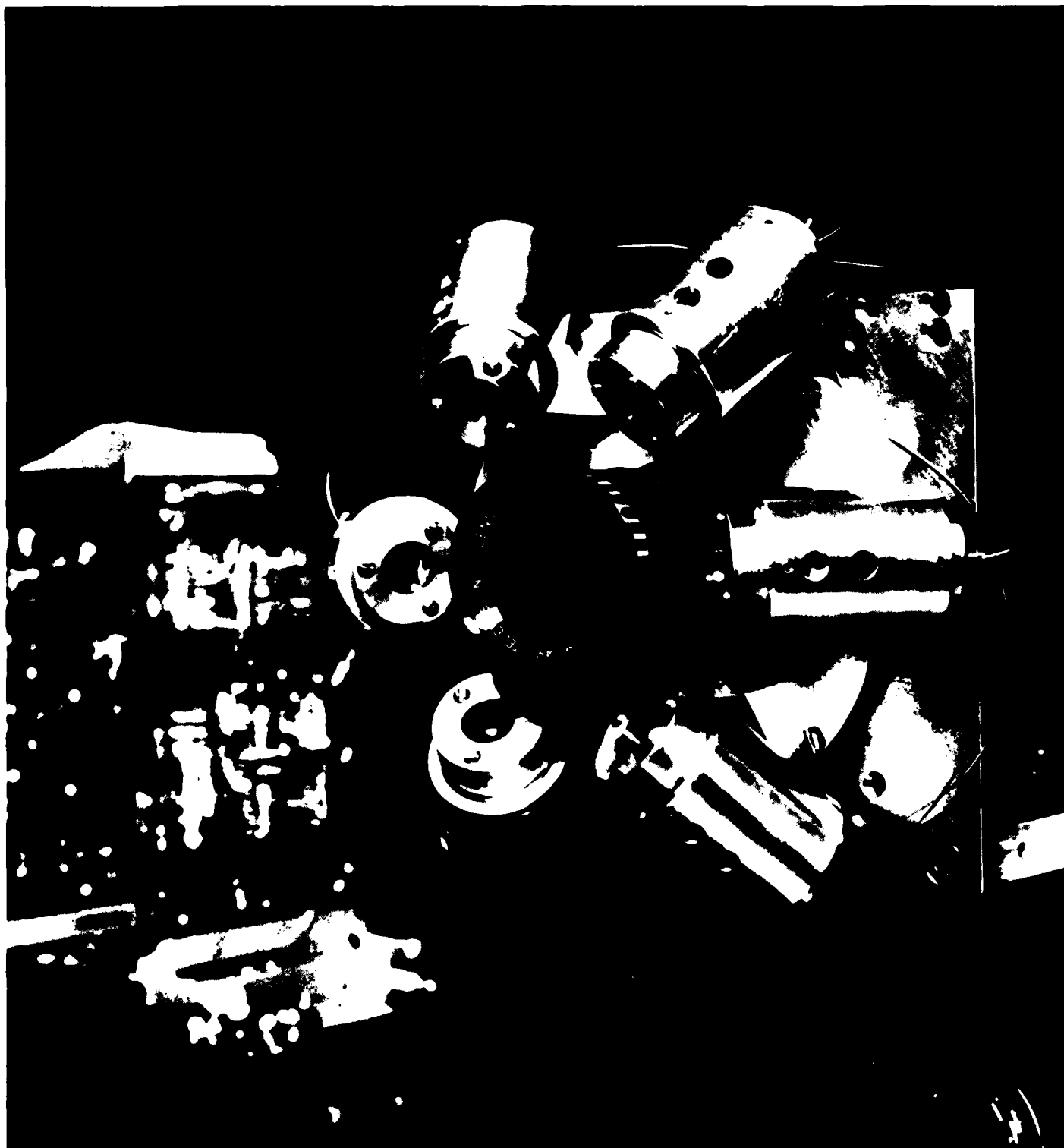
Figure 3: In this second version of the proximity sensor three light sources are focused towards one point on the optical axis, and three sources are focused towards a second point on the axis. As a result, this sensor can measure surface orientation throughout its linear range of 4 cm.
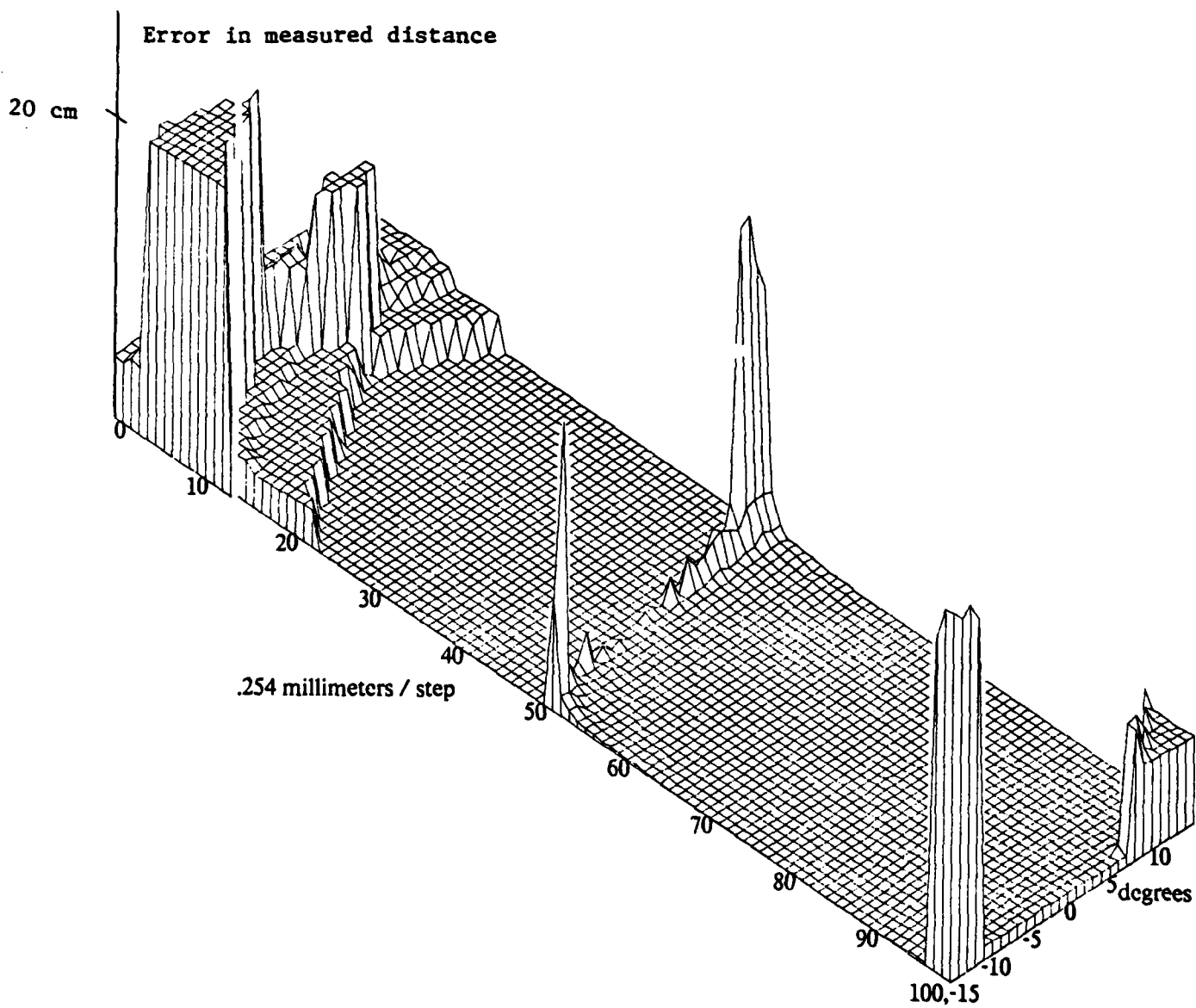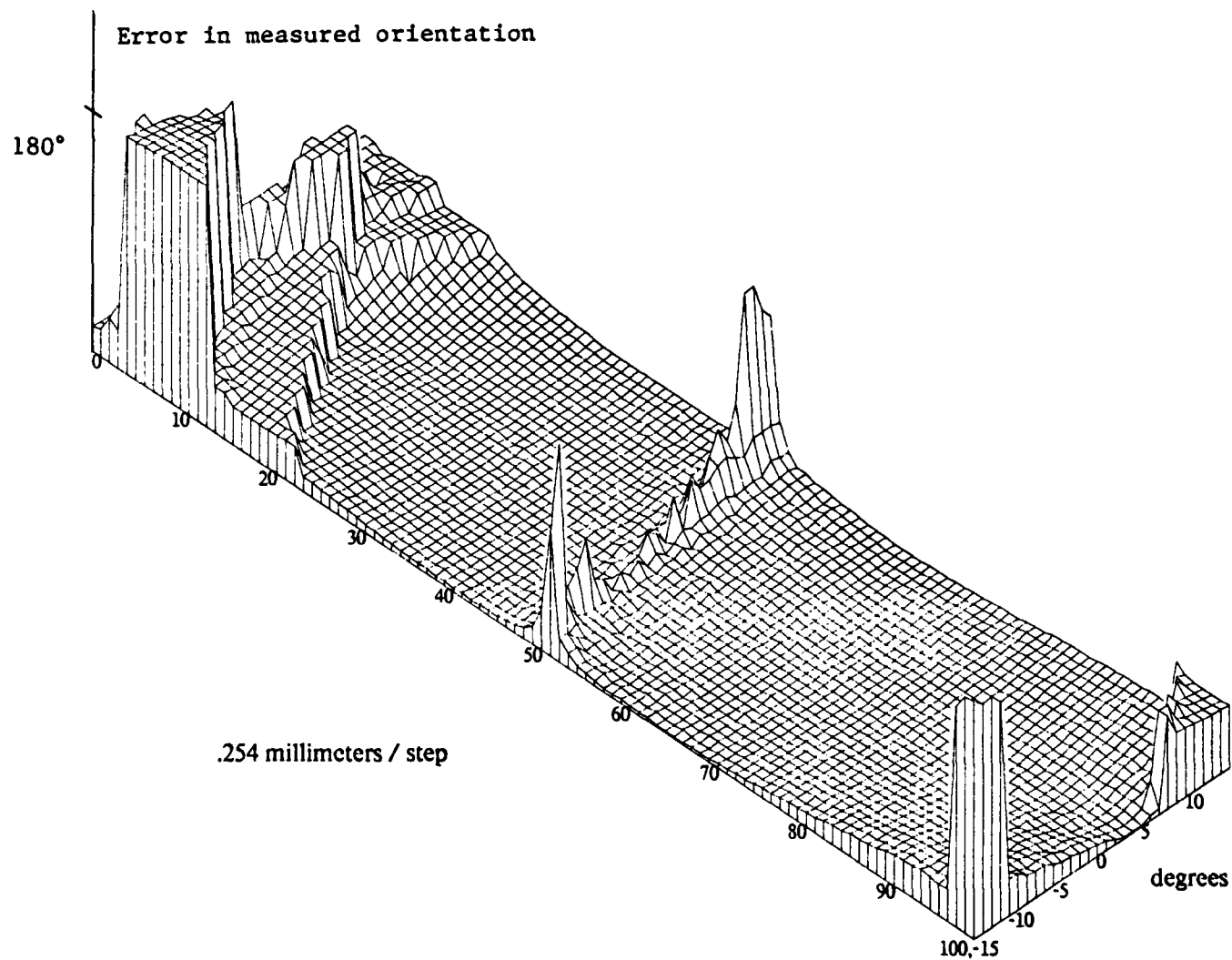
Figure 4: Figure 4(a) depicts the error in measured distance, and Figure 4(b) depicts the error in measured orientatation, as a function of the distance and orientation of the sensor with respect to a flat test surface.
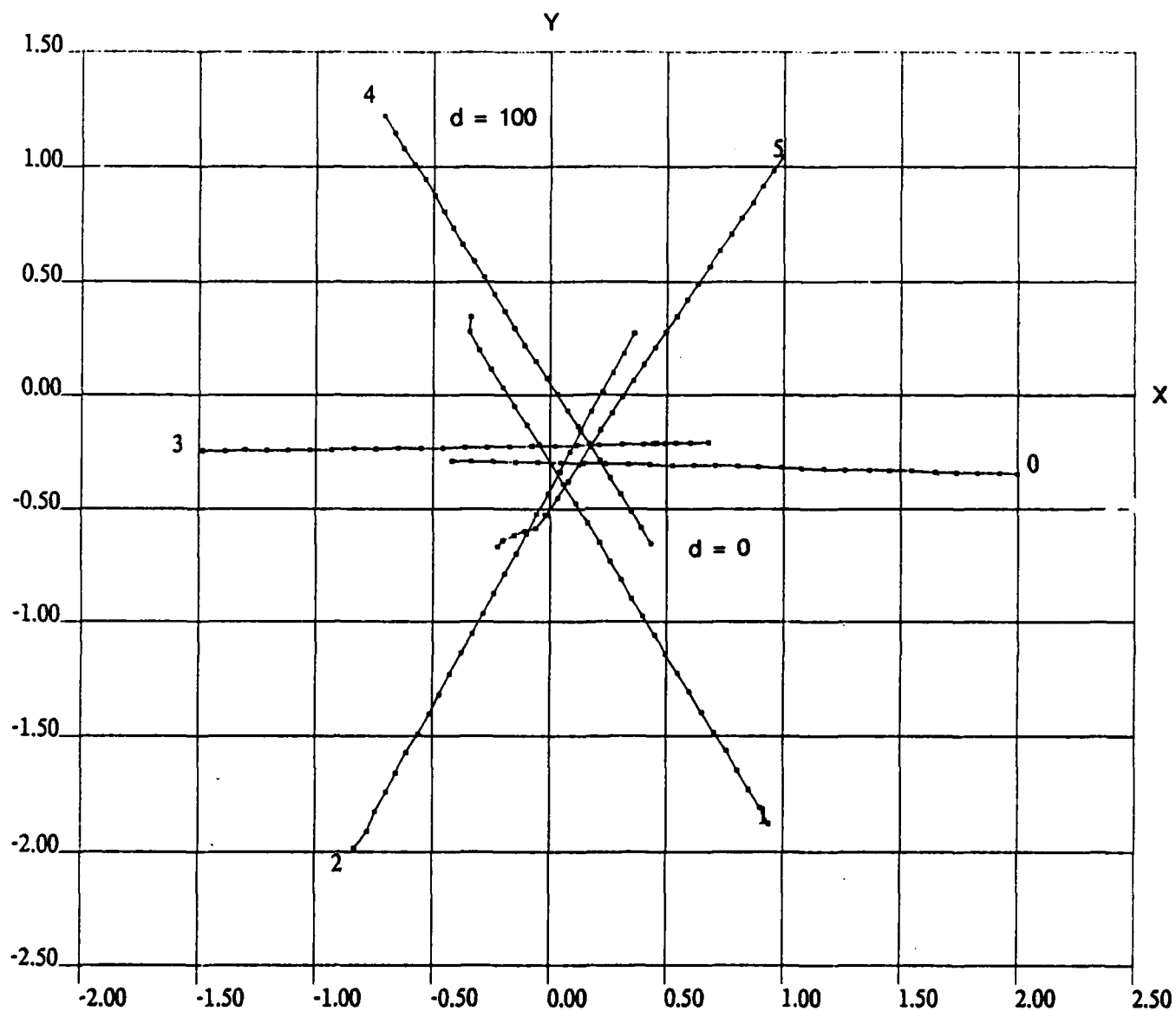
Error in measured orientation

180°

.254 millimeters / step

degrees

Figure 5: As a flat surface perpendicular to the sensor is moved along the optical axis the light spots on the surface follow individual trajectories. The sudden shift in the trajectory of light source number 5 occurs as the light spot leaves the field of view.
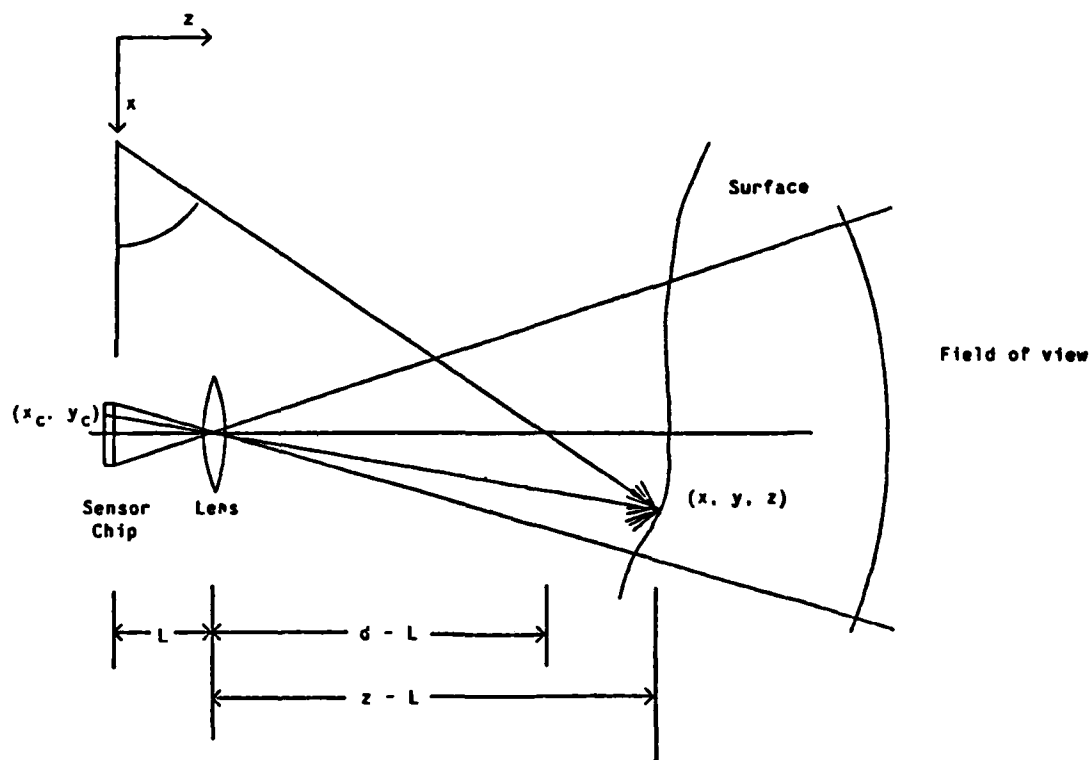
Figure 6: The relative positions of the sensor chip,
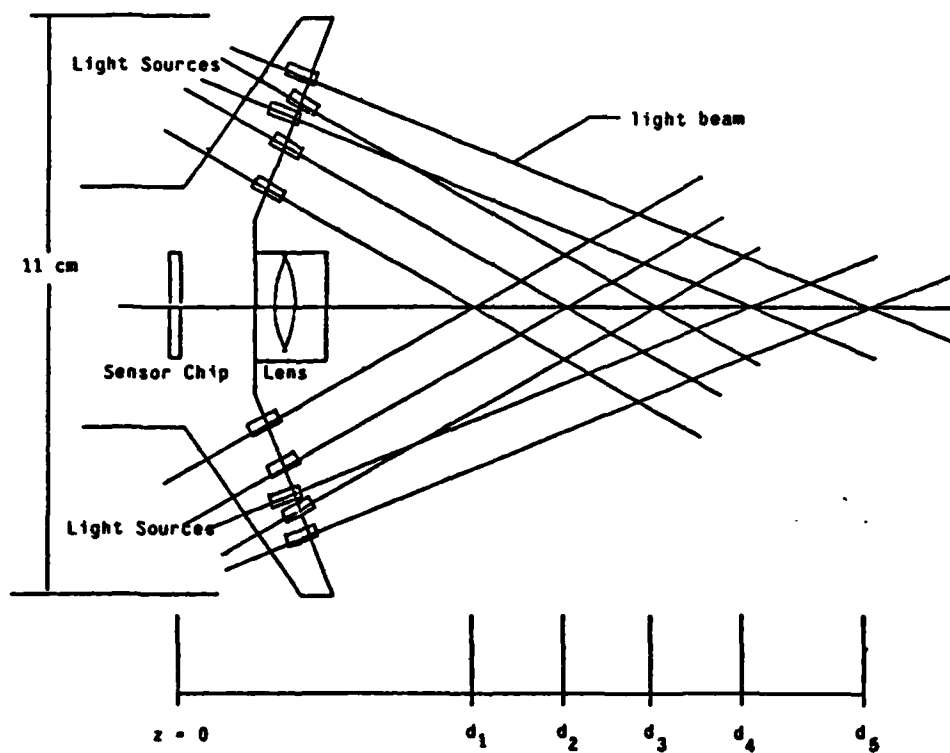the camera lens, and a light source.

Figure 7: The new proximity sensor is configured using multiple cones of light sources. The light beams are focused towards points along the optical axis.
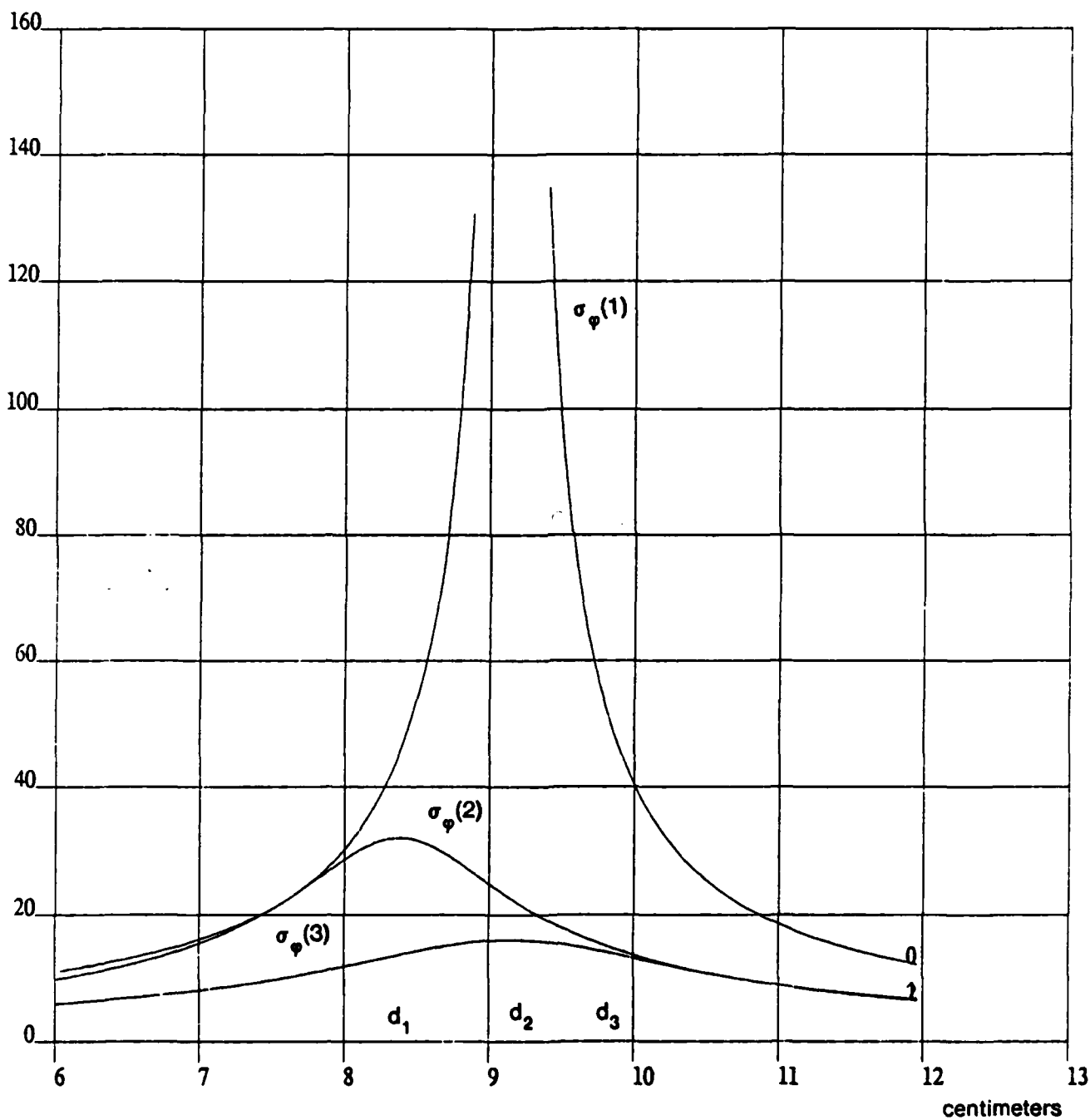
Figure 8: The uncertainty in the measured angular orientaion of a flat surface facing the proximity sensor perpendicularly is graphed as a function of distance according to equation(30). As additional conical rings of light sources are used the measurement accuracy increases.

END

FILMED

3-85

DTIC